ISSN: 2456-8473
International Journal of Chemistry, Pharmacy & Technology
Vol. 2, No.5, pp-185-192, 2017

GROWTH AND CHARACTERIZATION OF ZnO NANORODS (NRS) USING DIFFERENT PRECURSOR CONCENTRATIONS THE FIRST TIME ON POLYTETRAFLUOROETHYLENE (PTFE) SUBSTRATE

O.F. Farhat[1,2*], M.M. Halim[1], Naser M. Ahmed[1], A. A. Abuesamen[1] and M. A. Qaeed[3]

[1]Nano-Optoelectronics Research and Technology Laboratory, School of Physics, Universiti Sains Malaysia, 11800 Penang, Malaysia

[2]College of Arts and Sciences, Alasmarya Islamic University, Zliten, Libya

[3]Physics Department, Faculty of Education, Hodeidah University, Al Hodeidah, Yemen

Corresponding Author: omarfarhat67@yahoo.com

Received 23-04-17; Revised & Accepted: 27-05-17

ABSTRACT

ZnO nanorods (NRs) were successfully synthesized on PTFE substrates by a chemical bath deposition technique (CBD). The effects of precursor concentration on the growth of ZnO (NRs) were systematically characterized by X-ray diffraction (XRD), Field emission scanning electron microscopy (FESEM), Photoluminescence (PL), and Raman spectroscopy. The XRD results reveal that all the as-grown ZnO (NRs) arrays grew preferentially oriented along the c-axis with a hexagonal wurtzite structure. The FESEM images show that the ZnO (NRs) grown perpendicular to the PTFE substrates had lengths diameters ranging from 30 nm to 90 nm. PL and Raman analyses reveal that the aligned ZnO (NRs) exhibited a sharp ultraviolet peak E2 (high) at wave number between 437 and 438 cm^{-1}, respectively. Furthermore, the ZnO (NRs) grew vertically under 50 mM precursor concentration, resulting in a high structural and optical quality. These ZnO (NRs) can be potentially used for fabricating nano-electronics and nano-optical devices.

Keywords: ZnO(NRs); CBD; PTFE; Concentrations; FESEM; XRD

INTRODUCTION

The ZnO nanorod is a promising semiconductor material with a direct band gap (3.37 eV) and large binding energy (60 meV) at room temperature, high mechanical and thermal stabilities [1]. Therefore, several synthesis techniques such as atomic layer deposition, spin coating, molecular beam epitaxy (MBE) and chemical bath deposition have been developed to achieve these exceptional features [2-5]. The chemical bath deposition (CBD) method is an appropriate technique for the growth of ZnO (NRs) because it is a simple, low-temperature, low-cost, and scalable process [6,7]. This work has been done for the first time to study the effect of the different precursor concentration on the morphology and quality of ZnO (NRs) grown on PTFE substrates using CBD technique at low temperature. The optical and structural properties of the ZnO (NRs) produced on a seed-layer ZnO/PTFE substrate were investigated to determine the best concentration value effect on the synthesis of ZnO (NRs).

MATERIAL AND METHOD

The growth of ZnO (NRs) on ZnO seed-layer coated-Teflon (PTFE) substrates involved three steps. In the first stage is the Teflon substrates were firstly cut into square shapes with dimension of 2 cm × 2 cm. Then, to preparation of the ZnO and Zn seed layer, the Teflon substrate was cleaned ultrasonically by immersed it in isopropyl alcohol solution for 20 minute at 50℃. Finally, the Teflon substrate was washed in DI water and dried with nitrogen gas. In the second stage ZnO seed layer was grown on the cleaned PTFE substrates using radio frequency magnetron sputtering system with Argon pressure and sputtering power of 5.5 mTorr and 150 W, respectively. The result obtained with a 100 nm thick ZnO seed layer which is post-annealed in a furnace at 300 ^{o}C for 30 min. In the third stage the ZnO (NRs) were grown on the ZnO seed-layer/PTFE substrates using low-temperature chemical bath deposition (CBD) method, at different precursor concentrations. The amounts (10, 25, 50, 75 mM) of zinc nitrate hexahydrate ($Zn(NO_3)_2\_6H_2O$) were used and an equal molar concentration of hexamethylenetetramine ($C_6H_{12}N_4$) were separately dissolved in deionized water (DI). The prepared seed-layer ZnO/PTFE substrates were positioned vertically inside a beaker containing a mixture of two solutions. The beaker was placed in an oven for 3h at 95^{o}C for each concentration to study the effect of the precursor concentration on the growth of the ZnO (NRs). Finally, the samples were rinsed with hot DI water and dried with nitrogen gas. The surface morphology of the grown ZnO (NRs) was investigated by the field emission scanning electron microscope (FESEM) (model FEI/Nova NanoSEM450). The structure and growth orientation of ZnO nanorods were determined by X-ray diffraction (XRD) (PAN alytical X'Pert PROMRDPW3040). Raman spectroscopy (J obin Y von HR800UV) was used to investigate the structure of the ZnO nanorods at room temperature with an argon ion laser (514.5 nm) source, incident laser power of 20 mW and a system resolution of 1 cm^{-1}.

RESULTS AND DISCUSSION

The FESEM images of ZnO (NRs) array that were grown on PTFE substrates by using different precursor concentrations (10, 25, 50 and 75) mM is shown in Figures **(1)**. The hexagonal shapes of vertically aligned ZnO (NRs) are clearly noted. Unfortunately, cross section images of ZnO (NRs) prepared on PTFE substrate cannot be performed due to its flexibility. Figure (1) shows that the ZnO nanorod arrays synthesized on PTFE using a 10 mM precursor concentration, the ZnO nanorod size distribution shows a diameter ranging from 30 µm to 110 nm, with a mean value of 47 nm and a standard deviation value of 10. The mean value and the standard deviation were estimated from the (NRs) size normal distribution which is a very common continuous probability distribution. However, in Figure (b) the ZnO (NRs) synthesized using a precursor concentration of 25 mM exhibit a diameter ranging from 30 µm to100 nm with a mean value of 55 nm and a standard deviation value of 21. Figure 1 (c) shows that most of ZnO (NRs) grown using a precursor of 50 mM concentration exhibit a diameter ranging from 20 µm to 100 nm with an average mean value of 55 nm and a standard deviation value of 11. While the distribution of ZnO nanorod size that were grown using a precursor of 75 mM concentration shown in Figure 1(d) reveal a bigger (NRs) size from 60 µm to 130 µm with an average normal distribution mean value of 93 nm and a standard deviation value of 10. In comparison, the ZnO nanorod grown by using a precursor of 50 mM concentration have a relativity better morphology than the other samples, in addition to smaller and much uniform of it's (NRs) size.

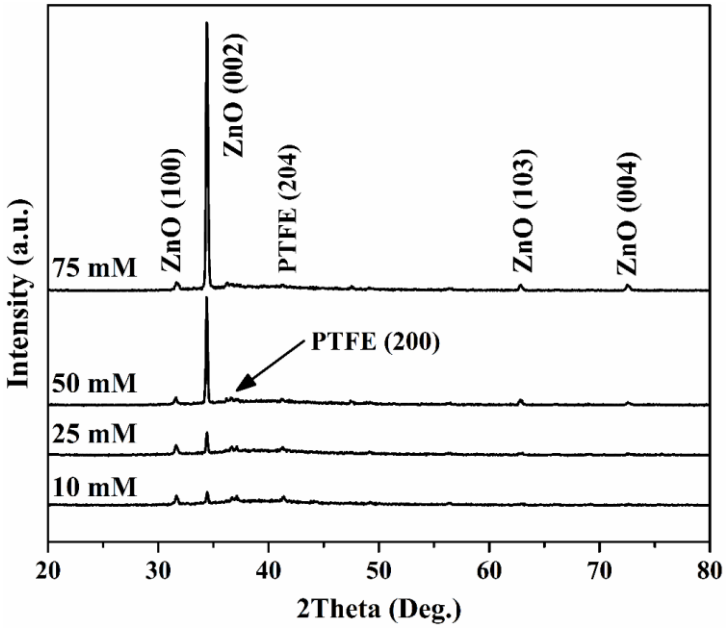

Fig. 1. XRD patterns of the ZnO nanorods with various precursor concentrations: (a) 10 mM, (b) 25 mM, (c) 50 mM, and (d) 75 mM.

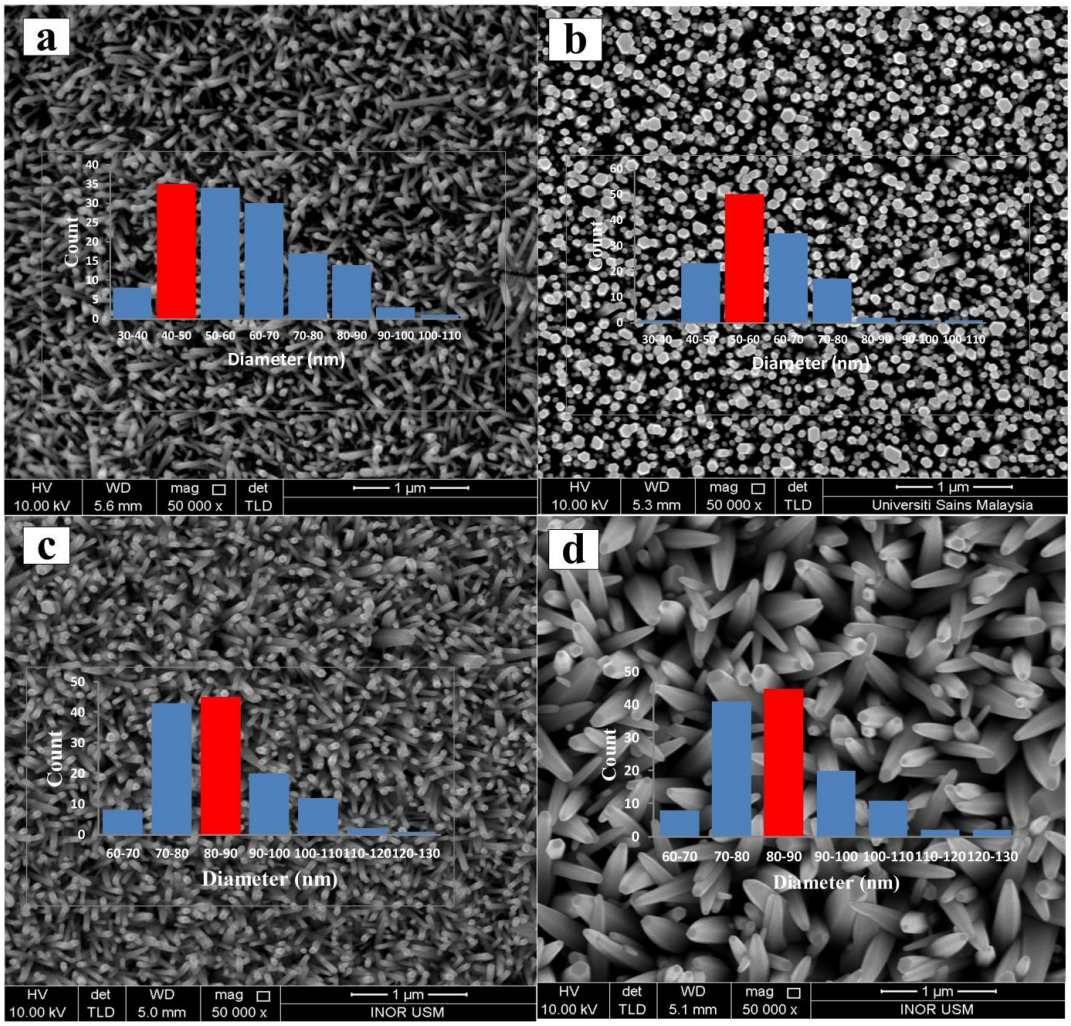

Fig. 2. FESEM images of the ZnO nanorod arrays with different precursor concentrations: (a) 10m M, (b) 25m M, (c) 50m M, and 75mM.

Figure 2 reveal the X-ray diffraction pattern of the ZnO (NRs) that were prepared by using precursor of different concentration and deposited on PTFE substrates respectively. The patterns of the prepared samples show four ZnO characteristic peaks around 2θ = 31.728°, 34.4°, 62.803° and 72.516° which were assigned for (100), (002), (103) and (004) crystal orientation respectively. The evaluated peaks were matched with ICDD reference code 01-080-0075. It should be noted here that the intensity of the peak at 34.4° increase significantly when using a precursor of higher concentration. The intense and sharp peaks appear at 34.4° reveal the growth of wurtzite hexagonal ZnO structure along the c-axis.

To analyze the crystalline quality of the synthesized ZnO (NRs), the lattice strain was calculated by using equation (1) [2]:

$$\varepsilon_c = \frac{c - c_0}{c_0} \qquad (1)$$

By taking the unstrained material have c_o=5.2098Å as in ICDD reference code 01-080-0075. Table shows the crystalline analysis of the XRD results for ZnO nanorod array that were prepared by using precursor of different concentration. The c-axis lattice parameter related to (002) orientation and the d-spacing were calculated by using Equations (2) and (3) respectively [8,9].

$$2d_{hkl} \sin\theta = n\lambda \qquad (2)$$

$$\frac{1}{d_{hkl}^2} = \frac{4}{3}\left(\frac{h^2 + hk + k^2}{a^2}\right) + \frac{l^2}{c^2} \qquad (3)$$

It is found that there is a light shift in the position of 2θ towards higher angle, this could be attributed to the lattice strain of ZnO nanostructure.

Table (1): X-ray diffraction analysis of ZnO nanorod grown on PTFE substrate from a precursor of different concentrations

Substrate	Conc.	2θ (Deg.)	d (Å)	c (Å)	ε_c
PTFE	10	34.410	2.60420	5.208	-0.027
	25	34.406	2.60452	5.209	-0.014
	50	34.405	2.60452	5.209	-0.014
	75	34.415	2.60383	5.208	-0.041

Figure 3 reveal the Raman spectra for ZnO (NRs) array that were prepared by using precursors of different concentration on PTFE substrate respectively. The detected Raman modes were only associated to ZnO wurtzite structure and the characteristic Raman peaks of PTFE substrates. There is no other peak(s) were detected, which confirm the growth of a pure phase of ZnO material. The detectable ZnO Raman mode (E_2 high) at wavenumber between 437 - 438 cm^{-1}. The intensity of the (E_2 high) found to enhance as the precursor concentration increases, which is in good agreement with XRD measurement. The domination of E_2 high mode indicating the sample has high crystal quality [10].

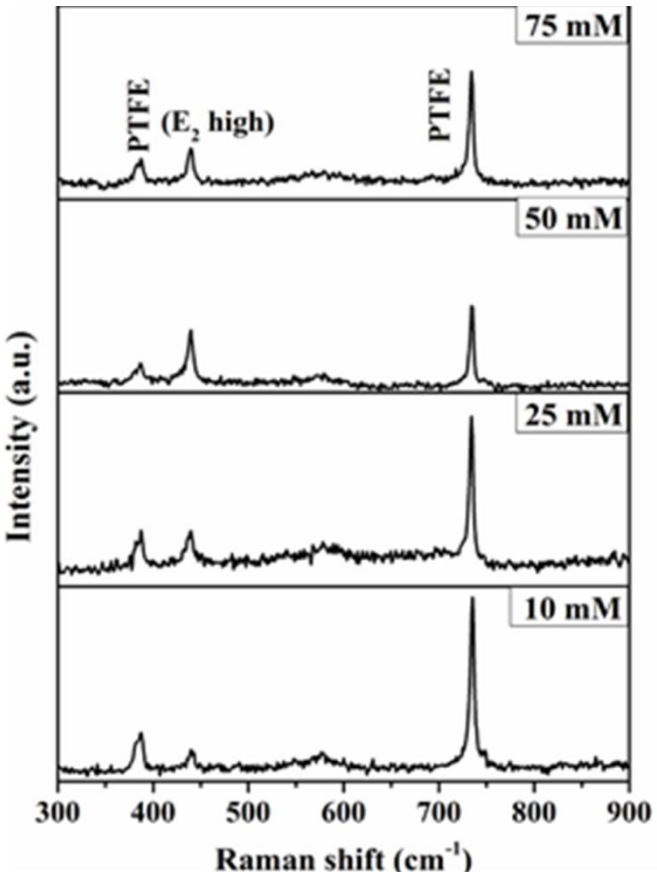

Fig 3. reveal the Raman spectra for ZnO nanorod array that were prepared by using precursors of different concentration on PTFE

The optical properties of as-grown ZnO (NRs) array were measured by Photoluminescence PL spectroscopy at room temperature (RT). Fig 4. shows the measured PL spectra form ZnO (NRs) prepared by using precursors with different concentrations on PTFE substrate. The ZnO PL spectra of all samples show three peaks, which were associated with ZnO emission bands. In all samples the domination peak observed in the UV region, which is assigned for the near band edge emission (NBE) of the wide bandgap of ZnO. This peak was located at 378 nm (3.28 eV), it has been attributed to the recombination of free exciton in ZnO material [11]. The PL spectra also shows a broad peak in the visible region in the wavelength ranging between (460 – 700) nm. This peak usually assigned for the deep emission levels (DE) of ZnO, which is related to the intrinsic or extrinsic defects in ZnO structure [12,13]. Finally, a small peak was detected at wavelength ≈ 760 nm which is assigned to the second order diffraction of the high intensity of UV emission band [14]. It should be noted here that the intensity of the UV emission band becoming more intense and sharp as the concentration of the deposition precursor increased indicating the growth of ZnO of better hexagonal structure. While the higher the ratio between the UV and VIS intensities I_{UV}/I_{VIS} is indicating the growth of ZnO structure having lower intrinsic and extrinsic defects.

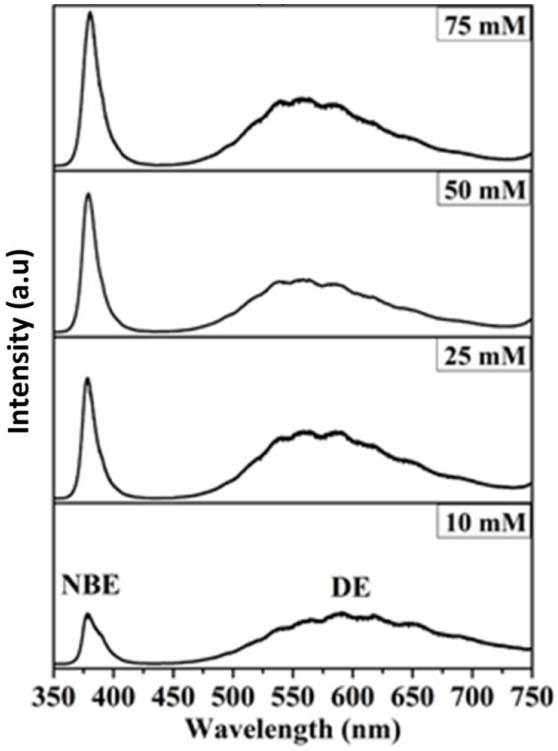

Figure 4**:** Photoluminescence (PL) of ZnO nanorod array grown from a precursor of different concentration on PTFE substrate.

Table 2 shows several data extracted the Photoluminescence PL spectra of ZnO nanorod grown on a PTFE substrate from a precursor of different concentrations. These data contain the center of the NBE peak position, NBE peak FWHM, and the ratio between the intensity of the band to band (NBE) emission and the defect emission (DE). The band gap of the fabricated ZnO nanorod was calculated from the extracted NBE peak position. The band gap of the ZnO nanorod show a stable value around (3.26 ±0.007) eV. Additionally, the full width at half maximum (FWHM) of the NBE emission peak revealed from ZnO nanorod prepared from a precursor of 50 mM concentration found to be the narrower compared to other samples, this indicates a lower defect density in 50 mM. The ratio of the NBE/DE peaks intensities found to be increased as the precursor concentration increase and again the 50 mM sample show the highest value confirming that the optimum concentration is 50 mM.

Table 2**:** Analysis data of the Photoluminescence spectra of ZnO (NRs) grown on PTFE substrate from a precursor of different concentrations.

Substrate	Concentration (mM)	NBE Position (nm)	Band gap (eV)	FWHM	(NBE/DE) Ratio
PTFE	10	380.8	3.256	15.28	0.632
	25	379.7	3.266	15.89	2.025
	50	379.6	3.267	12.94	4.474
	75	380.40	3.260	14.33	3.630

CONCLUSION

The effect of the precursor concentration on the morphology and the structural and optical properties of the aligned ZnO (NRs) grown using the CBD method at low temperature was systematically studied. Higher (002) peak in the XRD results confirmed the vertical growth of the

ZnO (NRs) from the PTFE substrate in the [002] direction along the c-axis. The low compressive stresses values showed the high-quality crystal structure of the aligned ZnO nanorods. The FESEM images indicate that the ZnO nanorod arrays grew vertically across the entire substrate. Furthermore, the diameters of the ZnO nanorod arrays increased with increasing precursor concentration. The room temperature PL spectra indicate that the vertical ZnO nanorods grown under 50 mM precursor concentration exhibited the sharpest. The good-aligned ZnO (NRs) grown on the PTFE substrates can be very suitable for applications photodetection devices.

Acknowledgments: We thank the Ministry of Higher Education, Malaysia for supporting this work under Grant 203/PSF/6721001. O.F. Farhat, acknowledges Alasmarya Islamic University for awarding him a scholarship to pursue his Ph.D. at USM.

REFERENCES

1. Shabannia, R. and H.A. Hassan, *Growth and characterization of vertically aligned ZnO nanorods grown on porous silicon: Effect of precursor concentration.* Superlattices and Microstructures, 2013. **62**: p. 242-250.
2. Farhat, O., et al., *ZnO nanofiber (NFs) growth from ZnO nanowires (NWs) by controlling growth temperature on flexible Teflon substrate by CBD technique for UV photodetector.* Superlattices and Microstructures, 2016. **100**: p. 1120-1127.
3. Carcia, P., R. McLean, and M. Reilly, *High-performance ZnO thin-film transistors on gate dielectrics grown by atomic layer deposition.* Applied physics letters, 2006. **88**(12): p. 123509.
4. Ilican, S., Y. Caglar, and M. Caglar, *Preparation and characterization of ZnO thin films deposited by sol-gel spin coating method.* Journal of optoelectronics and advanced materials, 2008. **10**(10): p. 2578-2583.
5. Look, D.C., et al., *Characterization of homoepitaxial p-type ZnO grown by molecular beam epitaxy.* Applied physics letters, 2002. **81**(10): p. 1830-1832.
6. Shabannia, R. and H. Abu-Hassan, *Vertically aligned ZnO nanorods synthesized using chemical bath deposition method on seed-layer ZnO/polyethylene naphthalate (PEN) substrates.* Materials Letters, 2013. **90**: p. 156-158.
7. Kim, M.S., et al., *Growth and characterization of seed layer-free ZnO thin films deposited on porous silicon by hydrothermal method.* Electronic Materials Letters, 2012. **8**(1): p. 75-80.
8. Farhat, O., et al., *Fabrication and characterization of ZnO nanowires by wet oxidation of Zn thin film deposited on Teflon substrate.* Superlattices and Microstructures, 2015. **86**: p. 236-242.
9. Farhat, O., et al., *Growth of vertically aligned ZnO nanorods on Teflon as a novel substrate for low-power flexible light sensors.* Applied Physics A, 2015. **119**(4): p. 1197-1201.
10. Zhang, R., et al., *Photoluminescence and Raman scattering of ZnO nanorods.* Solid State Sciences, 2009. **11**(4): p. 865-869.
11. Fonoberov, V.A., et al., *Photoluminescence investigation of the carrier recombination processes in ZnO quantum dots and nanocrystals.* Physical review B, 2006. **73**(16): p. 165317.

12. Dingle, R., *Luminescent transitions associated with divalent copper impurities and the green emission from semiconducting zinc oxide.* Physical Review Letters, 1969. **23**(11): p. 579.
13. Fonoberov, V.A. and A.A. Balandin, *Origin of ultraviolet photoluminescence in ZnO quantum dots: Confined excitons versus surface-bound impurity exciton complexes.* Applied physics letters, 2004. **85**(24): p. 5971-5973.
14. Tonon, C., et al., *Degradation of the optical properties of ZnO-based thermal control coatings in simulated space environment.* Journal of Physics D: Applied Physics, 2001. **34**(1): p. 124.